A combined Kalman-fractional calculus method for the parameter identification of structures under arbitrarily correlated ambient noise

K. Runtemund [1], **G. Cottone** [2], **G. Müller**[1]
[1] Technische Universität München, Chair of Structural Mechanics,
D-80333 München, Germany
e-mail: **katrin.runtemund@bv.tum.de**

[2] Technische Universität München, Engineering Risk Analysis Group,
D-80333 München, Germany

Abstract
In civil engineering forced vibration tests on structures such as bridges, long-span frame structures or buildings are usual costly and time consuming as they require a specific excitation by impact hammers or heavy shakers in order to excite the modes of interest with sufficient energy. Therefore often ambient vibration tests based on the 'natural' excitation of the structure due to wind or traffic loads are used, permitting to continuously measure the structural response without interruption of its use during large time intervals.
In order to study the dynamic behavior of structures computational efficient methods are required for: (i) the simulation of the loads and (ii) the estimation of the structural response to these loads using output-only model identification.
In this paper, we introduce a technique in which, first, the load is simulated by the recently proposed 'H-fractional spectral moments' (H-FSM) decomposition, which allows to represent a stationary colored Gaussian process in closed form as output of a system of linear fractional differential equations. Then, the identification of the model parameters and the system response is based on the H-fractional extended Kalman filter algorithm, a time domain approach which allows to consider uncertainties in the model of the structure as well as the autocorrelation of the process noise. The method is applied to a single degree of freedom system excited by different autocorrelated loads in order to estimate the stiffness and damping parameters.

1 Introduction

In the last four decades ambient vibration tests gained great attention in civil engineering. A literature review can be found e.g. in [1]. The first use of the ambient vibration technique for the dynamic characterization of full-scale structures is reported in the '70s. Since then the technique is extensively used in engineering in the scope of parameter identification (frequencies, damping ratios and modal shapes) [2, 3, 4, 5, 6, 7, 8], model updating [9, 8] as well as damage detection and health monitoring [10, 11, 12] of slender structures such as pedestrian bridges, chimneys, long-span frame structures or high-rise buildings. While forced vibration tests are in general costly, time consuming and often require a temporary out of service state of the structure, ambient vibration tests can be conducted using the excitation by natural and/or service loads as wind, traffic or humans. Such loads are caused by the superposition of multiple inputs and thus lead to a broad-band excitation of a significant number of vibration modes [13, 14]. Due to their inherent random nature, they have to be modeled as stochastic processes.
In the last years, many experimental modal identification methods for output-only measurements, such as the the peak picking method, the stochastic subspace identification method, the natural excitation technique have

been proposed. A comparative study on system identification techniques for the evaluation of the dynamic behavior of structures from ambient vibration test is given in [5].
All of these methods have in common that the load process is assumed to be white. However, in practical application where the power spectral density of the excitation is not constant within the system bandpass, the time-correlation of the load process is not negligible and thus the pure white noise assumption is not justified.In [15] a multi-dimensional Auto Regressive Moving Average (ARMA) parameter identification method is derived which allows to consider the excitation by sinusoidal loads, non-stationary white noise as well as colored noise with a rational spectrum. The latter property is also used in [16] where the state space model is augmented for correlated process noise using the spectral factorization theorem. It allows to model a wide sense stationary random process with PSD of rational form as an output of a linear system with white noise input. This system is then added to the original system by augmenting the state space representation leading to an overall linear system driven by white noise once again. The parameter identification can be then carried out with the help of the extended Kalman filter (EKF), a minimum variance estimator [17, 16].
Hence, the study of the dynamic behavior of the structure can be divided into two parts, namely the simulation of the random loads and the estimation of its response to these loads using output-only model identification methods.
Recently a new method for the representation of PSD and correlation function (AC) by means of a generalized Taylor expansion using fractional spectral moments (FSMs) was introduced in [18]. In contrast to common spectral fitting methods as AR, MA or ARMA models, where the coefficients are determined with respect to some optimization criteria and lack any further physical interpretation, the coefficients of the generalized Taylor series are derived in analytical form and have the meaning of spectral moments of non-integer type. The concept is used in [19] to derive a linear fractional differential equation, whose output is a stationary colored Gaussian process with target PSD, e.g. known from measurements. The method is called 'H-fractional spectral moments decomposition' as the coefficients for the noise simulation are calculated from the FSMs of the linear transfer function $H(\omega)$. In [20] it is applied for the simulation of wind loads and univariate/multivariate wind velocity fields, respectively.
Based on the H-FSMs decomposition the new issue presented in this paper is the derivation of a state space representation of arbitrarily correlated load processes in analytical form which neither require the factorization of the PSD nor any optimization procedure. Following the approach described in [16], the obtained state space model is augmented to the structural state space representation for the overall dynamic response analysis. As once again a linear system with white noise input is obtained, the extended Kalman filter can be applied for solving the parameter identification problem using output-only measurements of the system response.
In the following, the H-FSM method is described and some relevant applications in wind and ocean engineering are presented. Then, the Kalman filter algorithm is introduced and modified in order to include time-correlated process noise by state space augmentation. Here we will follow an approach given in [16] which uses the spectral factorization theorem for this purpose. The method is introduced for the validation of the developed generalized state space representation. Finally, the fractional algorithm is applied to a single degree of freedom system excited by the three load cases in order to estimate the stiffness and damping parameter of the system. A more detailed derivation of the proposed method can be found in [21].

2 Fractional representation of stationary Gaussian processes

2.1 Reconstruction of the PSD of correlated Gaussian processes by H-FSMs decomposition

In the following the main results of the method for the representation of colored Gaussian processes described in [19] are summarized for clarity's sake. Three load cases scenarios, i.e. process with exponential AC, von Kármán and Pierson Moskowitz PSD, are examined which are used throughout the paper for verification of the method.

Using this method the colored load process $\{F(t)\}$ with assigned PSD $S_F(\omega)$ is simulated as output of a linear differential equation excited by Gaussian white noise. This can be expressed using the a linear differential operator $\mathcal{L}(\cdot)$ in the form

$$\mathcal{L}(F(t)) = W(t) \tag{1}$$

where $\{W(t)\}$ denotes the zero-mean Gaussian white noise process. The corresponding input-output relation in terms of the PSD are given by

$$S_F(\omega) = |H(\omega)|^2 S_W(\omega) \tag{2}$$

where $H(\omega)$ is the transfer function and $S_W(\omega)$ denotes the PSD of zero-mean Gaussian white noise process $\{W(t)\}$ of intensity q_W characterized by the Fourier pair $S_W(\omega) = q_W/2\pi$ and $R(\tau) = E[W(t)W(t+\tau)] = q_W\,\delta(\tau)$. Assuming $Arg[H(\omega)] = 0$ the filter is defined from the target PSD

$$H(\omega) = |H(\omega)| = \sqrt{\frac{2\pi}{q_W} S_F(\omega)} \tag{3}$$

It must be noted that the assumption $Arg[H(\omega)] = 0$ leads to a non-causal system, i.e. $h(t) \neq 0$ for $t < 0$, hence, the generated time series of the process $\{F(t)\}$ is not just depending on the realizations $W(t_0)$, $W(t_{-1}), W(t_{-2}), ...$ of the white noise process $\{W(t)\}$ for $t < 0$ but also on future values $W(t_1), W(t_2), ...$ for $t > 0$. Nevertheless, due to the linearity of the underlying differential equation and the statistical independence of the Gaussian white noise process, the output remains a strict stationary Gaussian process.
The transfer function $H(\omega)$ and its Fourier transform can be reconstructed by H-fractional spectral moments (FSMs) defined as

$$\Pi_H(\gamma) = \int_{-\infty}^{\infty} H(\omega)\,|\omega|^{\gamma}\,\mathrm{d}\omega \tag{4}$$

as shown in [18]. The transfer function $h(t)$ and its Fourier transform $H(\omega)$ can be represented by

$$h(t) = \frac{1}{2\pi i}\int_{\rho-i\infty}^{\rho+i\infty} \nu(\gamma)\Pi_H(-\gamma)\,|t|^{-\gamma}\,\mathrm{d}\gamma. \tag{5}$$

$$H(\omega) = \frac{1}{4\pi i}\int_{\rho-i\infty}^{\rho+i\infty} \Pi_H(-\gamma)\,|\omega|^{\gamma-1}\,\mathrm{d}\gamma \tag{6}$$

where $\nu(\gamma) = \Gamma(\gamma)\cos(\gamma\pi/2)$. Both integrals are performed along the imaginary axis with fixed real part ρ which belongs to the fundamental strip of the Mellin transform calculated from Eq. (4). In some cases these contour integrals cannot be calculated in analytical form, but as the Gamma function $\Gamma(\gamma)$ decays exponentially fast in vertical strips, i.e. for $Im\gamma \to \infty$, depending on the decay of $\Pi_H(\gamma)$, the integrals might be truncated along the imaginary axis with constant real part $Re\gamma = \rho$ and approximated by their sums

$$h(t) \approx \frac{\Delta\eta}{2\pi}\sum_{k=-m}^{m} \nu(\gamma_k)\Pi_H(-\gamma_k)\,|t|^{-\gamma_k} \tag{7}$$

$$H(\omega) \approx \frac{\Delta\eta}{4\pi}\sum_{k=-m}^{m} \Pi_H(-\gamma_k)\,|\omega|^{\gamma_k-1} \tag{8}$$

Defining $\gamma_k = \rho + \mathrm{i}k\Delta\eta$, the integral is calculated up to a certain value $\bar{\eta} = \mp m\Delta\eta$ by discretizing the interval into $2m+1$ small increments $\Delta\eta$.

2.1.1 Numerical examples

Three load processes which are widely used in wind and ocean engineering are discussed.

1. Exponentially autocorrelated wind gusts

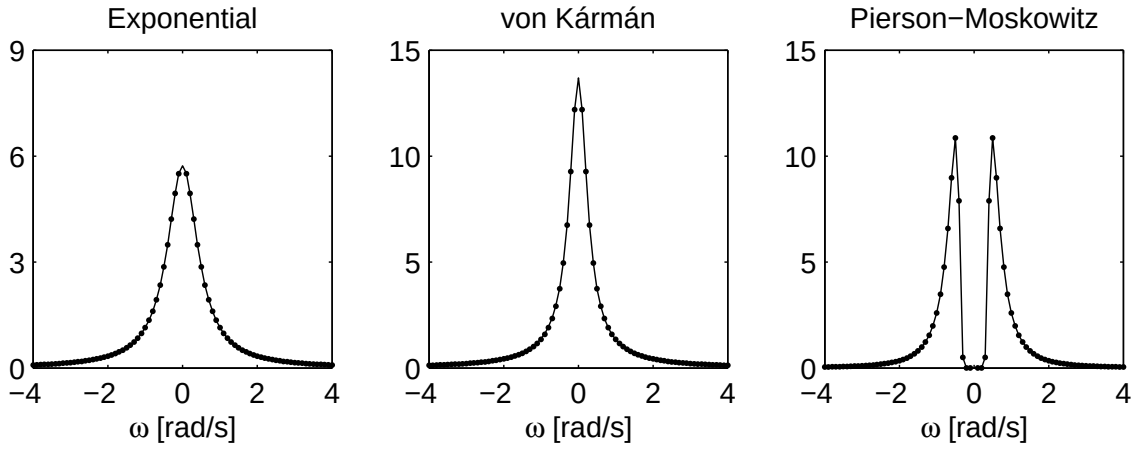

Figure 1: Exact (continuous) and approximated (dotted) power spectral densities for the three load cases: exponential AC, von Kármán and P-M PSD

The most simplest model for the description of along wind turbulences is a process with exponential AC function $R(\tau) = \sigma^2 e^{-a|t|}$ and corresponding rational low-frequency power spectrum $S_F(\omega)$ given by

$$S_F(\omega) = \frac{a\sigma^2}{\pi(a^2 + \omega^2)} \tag{9}$$

The H-FSMs of the transfer function $H(\omega) = \sqrt{2\pi S_F(\omega)/q}$ in Eq. (3) can be easily calculated by Mathematica leading to

$$\Pi_H(\gamma) = \left(\frac{1}{a^2}\right)^{-\gamma/2} \sqrt{\frac{2a\sigma^2}{q\pi}} \Gamma\left(-\frac{\gamma}{2}\right) \Gamma\left(\frac{1+\gamma}{2}\right); \qquad -1 < Re\gamma < 0 \tag{10}$$

The PSD $S_F(\omega)$ of the process is reconstructed by the relation $S_F(\omega) = |H(\omega)|^2 q/(2\pi)$. The approximation of the transfer function $H(\omega)$ in Eq. (8) is calculated choosing $a = 0.5$ [1/s], $\sigma = 3$ [N] and $\rho = 0.6$, $\Delta\eta = 0.2$ for the discretization of the integral involved taking into account $m = 20$ FSMs. From the results depicted in Fig. (1) it can be stressed that the proposed reconstruction leads to a good approximation of the analytic PSD. Moreover, the quality of the approximation depends solely on the chosen discretization of the integral given in Eq. (6).

2. Wind gusts with von Kármán velocity PSD

In general, if the PSD is rational it is not difficult to find a transfer function by spectral factorization [22, p. 180–195]. However, if the PSD of the process noise is given by a not rational function, there is no general method available for the analytically derivation of the transfer function $H(s)$ by spectral factorization and this is in fact a nontrivial task [23]. This is the case for the widely used von Kármán spectrum of along-wind turbulences given by

$$S_{Kar}(\omega) = \frac{\sigma^2 L}{\pi \bar{u}_z} \frac{1 + \frac{8}{3}\left(1.339 L \frac{\omega}{\bar{u}_z}\right)^2}{\left[1 + \left(1.339 L \frac{\omega}{\bar{u}_z}\right)^2\right]^{11/6}} \tag{11}$$

where σ, L is the standard deviation of the fluctuating component of the wind speed at height z and the integral turbulence scale lengths, respectively and $\bar{u}_z$ denotes the total velocity with which the assumed frozen-turbulence field propagates in space (Taylor's frozen-in turbulence hypothesis [24]). The PSD of the corresponding wind load is given by

$$S_F(\omega) = (\rho C_d A \bar{u}_z)^2 \, |\chi_a(z,\omega)|^2 S_{Kar}(\omega) \qquad \chi_a(z,\omega) = \left[1 + \left(\frac{2\omega\sqrt{A}}{\bar{u}_z}\right)^{4/3}\right]^{-1} \tag{12}$$

using the aerodynamic admittance $\chi_a(z,\omega)$ [25] and where ρ denotes the air density, C_d the drag coefficient, A the projected area of the structure and $\bar{u}(z)$ is the mean wind speed at hight z. Numerical values for the parameters for Germany can be taken e.g. from the national annexe of the "Eurocode 1: Actions on structures, Part 1-4: General actions/Wind actions" (DIN EN 1991-1-4:2010-12). In the example the parameters were chosen arbitrarily: $L = 10$ [m], $\sigma = 1$ [m/s], $z = 3$ [m], $\bar{u}_z = 18.25$ [m/s], $C_D = 1$, $A = 0.1$ [m^2] and $\rho = 1.25$ [kg/m]. The H-FSMs of the transfer function obtained can be calculated by introducing Eq. (12) into Eq. (3) using Mathematica. This leads to

$$\Pi_H(\gamma) = C(\gamma) + \sum_{k=0}^{2} \frac{D\Gamma[\frac{5+2c_k}{12}]\Gamma[\frac{-1}{6c_k}]_3F_2[1, \frac{2c_k+5}{24}, \frac{2c_k+17}{24}; \frac{c_k+6}{12}, \frac{c_k+12}{12}, \frac{-b^2L^4}{A^2}]\bar{u}_z^{\frac{3}{2}+\gamma}}{(-1)^k b^{\frac{-1}{6c_k}} \bar{A}^{\frac{2(1+k)}{3}} L^{\frac{-c_k}{3}} \Gamma[\frac{5}{12}]} \tag{13}$$

for $-1 < Re\gamma < 7/6$ with

$$C(\gamma) = -\frac{3i\pi D\bar{A}^{-\frac{1+\gamma}{2}} e^{\frac{3i\pi(1+\gamma)}{4}} (-ie^{\frac{3i\pi\gamma}{2}}(1 - \frac{ibL^2}{\bar{A}})^{\frac{5}{12}} + (1 + \frac{ibL^2}{\bar{A}})^{\frac{5}{12}})\bar{u}_z^{\frac{3}{2}+\gamma}}{(1 + e^{3i\pi\gamma})(1 + \frac{b^2L^4}{A^2})^{\frac{5}{12}}}$$

where $c_k = 1 + 4k - 3\gamma$, $b = 70.8$, $\bar{A} = 4A$, $D = \sqrt{8\pi L(AC_d\sigma\rho)^2/q}$ and ${}_pF_q[a_1, ...a_p; b_1, ...b_q; z]$ is the generalized hypergeometric function. The analytical form of the H-FSMs leads, also in this case, to a very efficient application of the method. In Fig. (1) the results are illustrated having chosen the following parameters: $\rho = 0.6$, $\Delta\eta = 0.15$, $m = 30$.

3. Wind waves with Pierson Moskowitz PSD

In this last example the process noise is generated from a wind wave PSD of fully developed sea introduced by Pierson and Moskowitz (P-M). It was developed on the basis of 460 spectrums obtained from measurements in the North Atlantic Ocean from 1955 to 1960 and is given by

$$S_{PM}(\omega) = \frac{a}{\omega^5} e^{-\frac{b}{\omega^4}} \tag{14}$$

where $a = 0.0081g^2$, $b = 0.74(g/\bar{u}_{19.5})^4$ and g is the acceleration due to gravity. Assuming a stationary process the wave force acting on a vertical pile with diameter D at hight z is given by

$$S_F(z,\omega) = \left(\frac{8}{\pi}\sigma_u^2 K_d^2 + K_1^2\omega^2\right)\left(\frac{\omega\cosh(k(z+h))}{\sinh(kh)}\right)^2 S_{PM}(\omega) \tag{15}$$

with $K_d = 1/2\rho C_d D$, $K_1 = \rho C_m \pi D^2/4$ and where k is the angular wave number, h the water depth, ρ is the density of the sea water, C_m is the inertia coefficient and σ_u is the standard deviation of the fluid particle velocity [26]. In general C_m ranges between $1.6 - 2.5$ and for a vertical cylinder $C_m = 2.0$ can be assumed. The drag coefficient C_d never falls below 0.6 and for a smooth cylinder $C_d = 1.0$ [27]. Eq. (15) is valid for non-breaking waves and when the dimension of the structure is small compared to the wave length λ, i.e. when $D < 0.2\lambda$. A detailed description of the derivation of Eq. (15) can be found in [26]. The H-FSMs are given, also in this case, in analytical form

$$\begin{aligned}\Pi_H(\gamma) = \frac{2^{c-2}}{b^{\frac{1}{8}}}\sqrt{\frac{a\cosh[k(h+z)]^2}{Aq\sinh[hk]^2}}\Bigg(&Ab^{\frac{\gamma}{4}}\sqrt{8\pi}\Gamma[c]{}_2F_2\left[-\frac{1}{4},\frac{1}{4};\frac{1}{2},1-c,-\frac{bB^2}{2A^2}\right] + \\ &+ b^{\frac{5}{8}-c}B\sqrt{\pi}\Gamma\left[c-\frac{1}{2}\right]{}_2F_2\left[\frac{1}{4},\frac{3}{4};\frac{3}{2},\frac{3}{2}-c;-\frac{bB^2}{2A^2}\right] - 2^{\frac{3}{2}-c}b^{\frac{1}{8}}A^{1-2c}B^{2c} \\ &\Gamma\left[2c-\frac{1}{2}\right]\Gamma[-2c]{}_2F_2\left[c-\frac{1}{4},c+\frac{1}{4};c+\frac{1}{2},c+1;-\frac{bB^2}{2A^2}\right]\Bigg)\end{aligned} \tag{16}$$

for $Re\gamma < -1/2$ and $c = 1/8 - \gamma/4$, A=$8/\pi\sigma_u^2K_d^2$ and $B = K_1^2$. In the example a pile with diameter $D = 0.1$ [m], drag coefficient $C_d = 0.6$ and inertia coefficient $C_m = 2$ which is excited by wind-induced ($\bar{u}_{19.5} = 20$ [m/s], $\sigma_u = 1$ [m/s]) ocean waves with wave length $\lambda = 20$ [m] and water depth $h = 15$ [m] is assumed. The corresponding PSD of the wave loads and the approximation using $m = 40$ FSMs and $\rho = 1.6$, $\Delta\eta = 0.3$ for the discretization of the integral involved is depicted in Fig. (1). Once again a good agreement between the approximated and the exact PSD is obtained.

2.2 Digital simulation of the load process

The obtained fractional representation of the transfer function $H(\omega)$ can be now used for a reconstruction of the correlated noise process $\{F(t)\}$ in terms of the H-FSMs given by [20]

$$F(t) = \frac{1}{4\pi i} \int_{\rho - i\infty}^{\rho + i\infty} \Pi_H(-\gamma)(I^{1-\gamma} W)(t) \mathrm{d}\gamma \tag{17}$$

where $(I^{\gamma} f)(t)$ denotes the Riesz fractional integral. The integral representation of the colored load process defined in Eq. (17) can be approximated by the truncated sum

$$F(t) \approx \frac{\Delta\eta}{4\pi} \sum_{k=-m}^{m} \Pi_H(-\gamma_k)(I^{1-\gamma_k} W)(t) \tag{18}$$

Hence, the main difficulty in the simulation of the process lies in the efficient calculation of the Riesz fractional integral $(I^{1-\gamma_k} W)(t)$ of the Gaussian white noise process $\{W(t)\}$. It can be shown that the Grünwald - Letnikov form of the Riesz fractional integral is given by:

$$(I^{\gamma} W)(j\tau) \approx \lim_{\tau \to +0} \sum_{k=0}^{j} \alpha_k(\gamma) W(j\tau - k\tau) + \lim_{\tau \to +0} \sum_{k=0}^{n-j} \alpha_k(\gamma) W(j\tau + k\tau) \tag{19}$$

where

$$\alpha_k(\gamma) = \frac{(-1)^k \tau^{\gamma-1}}{2\cos(\gamma\pi/2)} \binom{-\gamma}{k} \tag{20}$$

As shown in [20] Eq. (19) can be calculated efficiently in matrix form by $\mathbf{Z}(\gamma) = \mathbf{A}(\gamma)\mathbf{W}$

$$\mathbf{Z}(\gamma) = \begin{bmatrix} (I^{\gamma} W)(0) \\ (I^{\gamma} W)(\tau) \\ \dots \\ (I^{\gamma} W)(n\tau) \end{bmatrix}; \quad \mathbf{A}(\gamma) = \begin{bmatrix} 2\alpha_0 & \alpha_1 & \dots & \alpha_n \\ \alpha_1 & 2\alpha_0 & \dots & \dots \\ \dots & \dots & \dots & \alpha_1 \\ \alpha_n & \dots & \alpha_1 & 2\alpha_0 \end{bmatrix}; \quad \mathbf{W} = \begin{bmatrix} W(0) \\ W(\tau) \\ \dots \\ W(n\tau) \end{bmatrix} = \begin{bmatrix} G_0 \\ G_1 \\ \dots \\ G_n \end{bmatrix} \tag{21}$$

where the discretized white noise process $\mathbf{W}$ in the interval $[0, n\tau]$ is described by the realizations of a zero-mean Gaussian random process $G_0, G_1, \dots, G_n$ with standard deviation $\sqrt{q\tau}$. The vector of the colored load process $\mathbf{F} = [F(0), F(\tau), \dots, F(n\tau)]^T$ is finally obtained by

$$\mathbf{F} = \frac{\Delta\eta}{4\pi} \sum_{k=-m}^{m} \Pi_H(-\gamma_k)\mathbf{Z}(1-\gamma_k) = \sum_{k=-m}^{m} \mathbf{h}(\gamma_k)\mathbf{W} \tag{22}$$

by means of the matrix transfer function $\mathbf{h}(\gamma_k) = \Delta\eta(4\pi)^{-1}\Pi_H(-\gamma_k)\mathbf{A}(1-\gamma_k)$. A verification of the result in Eq. (22) by means of the three load cases can be found in [21].

2.2.1 Generalized state space representation of colored random processes

Based on the result given in Eq. (22) we will now develop a general state space representation for colored load processes. It must be stressed that it is valid for arbitrary correlated Gaussian processes and can be given directly once the H-FSMs in Eq. (4) are calculated.

Due to the Toeplitz form of the coefficient matrix $\mathbf{A}(\gamma)$ the matrix transfer function $\mathbf{h}(\gamma_k)$ in Eq. (22) can be calculated easily. Furthermore, if $Re\gamma > -1$ is chosen, then the coefficients $\alpha_k(\gamma)$ decrease with inverse power law behavior as k increases and can be neglected in this case after a finite number of terms p, which mainly depends on the decay of the correlation function. It must be noted that for an input vector $\mathbf{W}$ of length n, the first and last p samples of the output $\mathbf{F}$ can be regarded as the 'transition states' whereas the remaining $n - 2p$ samples are the 'steady states' which are needed in the following for the formulation of a

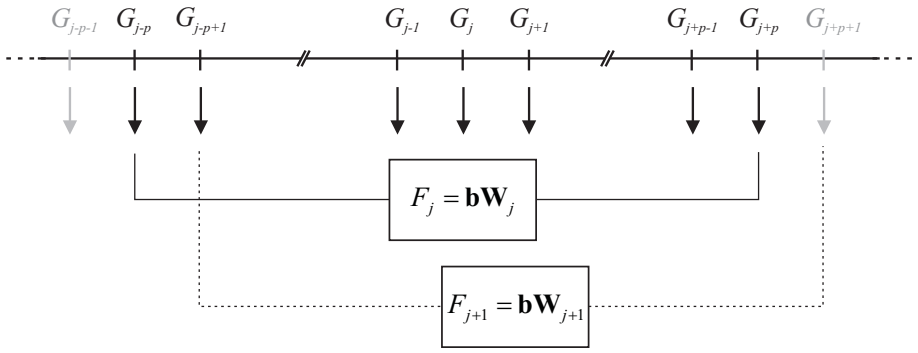

Figure 2: Steady state realization of the load process: the load F_{j+1} of the next time step is generated by shifting the p-dimensional vector $\mathbf{W}_j$ of increments of white noise

recursive state space form. The calculation of one steady state realization $F_j = F(j\tau)$ of the discrete load process $\mathbf{F}$, with $j = 0, 1, \ldots, n$ is given by

$$F_j = \frac{\Delta\eta}{4\pi} \sum_{k=-m}^{m} \Pi(-\gamma_k) \begin{bmatrix} \alpha_p(1-\gamma_k) \\ \alpha_{p-1}(1-\gamma_k) \\ \cdots \\ 2\alpha_0(1-\gamma_k) \\ \cdots \\ \alpha_{p-1}(1-\gamma_k) \\ \alpha_p(1-\gamma_k) \end{bmatrix}^T \begin{bmatrix} G_{j-p} \\ G_{j-p+1} \\ \cdots \\ G_j \\ \cdots \\ G_{j+p-1} \\ G_{j+p} \end{bmatrix} = \begin{bmatrix} \beta_p \\ \beta_{p-1} \\ \cdots \\ 2\beta_0 \\ \cdots \\ \beta_{p-1} \\ \beta_p \end{bmatrix}^T \begin{bmatrix} G_{j-p} \\ G_{j-p+1} \\ \cdots \\ G_j \\ \cdots \\ G_{j+p-1} \\ G_{j+p} \end{bmatrix} \tag{23}$$

where

$$\beta_p = \frac{\Delta\eta}{4\pi} \sum_{k=-m}^{m} \Pi_H(-\gamma_k)\alpha_p(1-\gamma_k) \tag{24}$$

as illustrated in Fig. (2). As one can see from Eq. (23) the actual sample $F_j = \mathbf{bW}_j$ of the load process is calculated by the time-invariant vector $\mathbf{b} = [\beta_p, \beta_{p-1}, ..., 2\beta_0, ..., \beta_{p-1}, \beta_p]$ including the weights of the $(2p+1)$ elements of the vector of the white input noise $\mathbf{W}_j = [G_{j-p}, ..., G_j, ..., G_{j+p}]$ consisting out of the p previous and past samples of the Gaussian noise process. This allows to formulate a recursive state space representation, which is needed later in order to include the colored noise process $\{F(t)\}$ into the Kalman filter algorithm, by a forward shift of the white noise process as shown in Fig. (2). This leads to the following state space form

$$\mathbf{x}'_{k+1} = \mathbf{A}_d\mathbf{x}'_k + \mathbf{B}_d w_k \qquad F_k = \mathbf{C}_d\mathbf{x}'_k \tag{25}$$

where $\mathbf{x}'_k = [G_{k-p}, G_{k-p+1}, ..., G_k, ..., G_{k+p-1}, G_{k+p}]^T$ and with time-invariant transfer matrices $\mathbf{A}_d$, $\mathbf{B}_d$ and $\mathbf{C}_d$

$$\mathbf{A}_d = \begin{bmatrix} 0 & 1 & 0 & \ldots & \ldots & 0 & 0 \\ \ldots & 0 & 1 & 0 & \ldots & \ldots & 0 \\ \ldots & \ldots & 0 & 1 & 0 & \ldots & \ldots \\ \ldots & \ldots & \ldots & 0 & \cdots & \ldots & \ldots \\ \ldots & \ldots & \ldots & \ldots & \ldots & \ldots & \ldots \\ 0 & \ldots & \ldots & \ldots & \ldots & 0 & 1 \\ 0 & 0 & \ldots & \ldots & \ldots & 0 & 0 \end{bmatrix} \qquad \mathbf{B}_d = \begin{bmatrix} 0 \\ 0 \\ \ldots \\ \ldots \\ \ldots \\ 0 \\ 1 \end{bmatrix} \qquad \mathbf{C}_d = \begin{bmatrix} \beta_p \\ \beta_{p-1} \\ \cdots \\ 2\beta_0 \\ \cdots \\ \beta_{p-1} \\ \beta_p \end{bmatrix}^T \tag{26}$$

In the following the subindex d for discrete-time will be omitted for simplicity of notation. It shall be highlighted that Eq. (25) is a general state space representation of stationary arbitrarily colored load processes with known PSD. Once, the H-FSM of the PSD are determined using Eq. (4) the corresponding state space form is defined by Eq. (25).

Time Update (Prediction)	Measurement Update (Correction)
Prior estimate $\bar{\mathbf{x}}_{k+1} = \mathbf{T}\mathbf{x}_k$	Kalman gain matrix Posterior estimate $\mathbf{K}_k = \bar{\Sigma}_{xx_{k+1}}\mathbf{H}^T(\Sigma_{vv_k} + \mathbf{H}\bar{\Sigma}_{xx_{k+1}}\mathbf{H}^T)^{-1}$
Prior error covariance: $\bar{\Sigma}_{xx_{k+1}} = \mathbf{T}\Sigma_{xx_k}\mathbf{T}^T + \mathbf{S}\Sigma_{ww_k}\mathbf{S}^T$	Posterior estimate $\mathbf{x}_{k+1} = \bar{\mathbf{x}}_{k+1} + \mathbf{K}_k(\mathbf{z}_{k+1} - \mathbf{H}\bar{\mathbf{x}}_{k+1})$
	Posterior error covariance $\Sigma_{xx_{k+1}} = \bar{\Sigma}_{xx_{k+1}} - \mathbf{K}_k\mathbf{H}\bar{\Sigma}_{xx_{k+1}}$

Table 1: Kalman filter algorithm

3 Kalman filter algorithm for correlated process noise

The Kalman filter was developed in 1960 by Rudolf Kálmán [17]. It is an optimal recursive algorithm to estimate the state $\mathbf{x} \in \mathbb{R}^n$ of a linear dynamic system discretized in the time domain using noisy measurement data $\mathbf{z} \in \mathbb{R}^m$. The discretized state space model of a system excited by a Gaussian white noise process $\mathbf{w}$ is generated by two equations, the system and measurement equation

$$\mathbf{x}_{k+1} = \mathbf{T}\mathbf{x}_k + \mathbf{S}\mathbf{w}_k \qquad \mathbf{z}_k = \mathbf{H}\mathbf{x}_k + \mathbf{v}_k \tag{27}$$

where $\mathbf{T} \in \mathbb{R}^{n\times n}$, $\mathbf{S} \in \mathbb{R}^{n\times u}$ and $\mathbf{H} \in \mathbb{R}^{m\times n}$ are the transfer matrices and $\mathbf{w}_k \in \mathbb{R}^u$ and $\mathbf{v}_k \in \mathbb{R}^m$ are uncorrelated stationary zero-mean white noise processes. The transfer matrix $\mathbf{T}$ relates the actual state k to the state at the next time step $k+1$. The model uncertainties or unmeasured disturbances are represented by the added m-dimensional noise vector $\mathbf{w}_k$ which is related to the actual state by the matrix $\mathbf{S}$. The KF is based on a Gaussian noise model, i.e. the measurement error $\mathbf{v}_k \propto N(\mathbf{0}, \mathbf{\Sigma}_{vv,k})$ as well as the state error $\mathbf{w}_k \propto N(\mathbf{0}, \mathbf{\Sigma}_{ww,k})$ are modeled as independent, white noises with normal distribution where $\mathbf{\Sigma}_{vv,k} \in \mathbb{R}^{m\times m}$, $\mathbf{\Sigma}_{ww,k} \in \mathbb{R}^{n\times n}$ denote the measurement and process noise covariance matrix, respectively. The algorithm is characterized by an iterative prediction-correction structure as shown in Tab. (1). In the *prediction step* a time update of the current state $\mathbf{x}_k$ and error covariance matrix $\mathbf{\Sigma}_{xx,k}$ is taken in order to obtain a prior estimate of the process state $\bar{\mathbf{x}}_{k+1}$ and its associated error covariance matrix $\bar{\mathbf{\Sigma}}_{\bar{x}\bar{x},k+1}$ of the next time step. The time-update of the current state is calculated from the undisturbed system equation $\bar{\mathbf{x}}_{k+1} = \mathbf{T}\mathbf{x}_k$ where the prediction error leads to the update of the covariance matrix and where the tilde indicates the true state

$$\begin{aligned} \epsilon_{\bar{x},k+1} &= \tilde{\mathbf{x}}_{k+1} - \bar{\mathbf{x}}_{k+1} = \mathbf{T}(\tilde{\mathbf{x}}_k - \mathbf{x}_k) + \mathbf{S}(\tilde{\mathbf{w}}_k - \mathbf{w}_k) \\ \mathbf{\Sigma}_{\bar{x}\bar{x},k+1} &= E[\epsilon^T_{\bar{x},k+1}\epsilon_{\bar{x},k+1}] = \mathbf{T}\mathbf{\Sigma}_{xx,k}\mathbf{T}^T + \mathbf{S}\mathbf{\Sigma}_{ww,k}\mathbf{S}^T \end{aligned} \tag{28}$$

In the *correction step* the measurement equation is used to predict the likeliest measurement for the given prior state estimate. Once the actual measurement is obtained, the difference $\mathbf{d}_k = \mathbf{H}\bar{\mathbf{x}}_k - \mathbf{z}_k$ between the predicted measurement and the actual measurement, also known as innovation or residual, is calculated. The Kalman gain matrix $\mathbf{K}_k$ is determined in order to correct the prior state estimate $\bar{\mathbf{x}}_{k+1}$ in the measurement update. It is the result of the minimization of the mean-square error of the posterior state estimate $\mathbf{x}_{k+1}$

$$\epsilon_{x,k+1} = \tilde{\mathbf{x}}_{k+1} - \mathbf{x}_{k+1} \qquad E[\epsilon^T_{x,k+1}\epsilon_{x,k+1}] \rightarrow min. \tag{29}$$

It leads to the Kalman gain matrix $\mathbf{K}_k$ which is used to calculate the optimal estimate $\mathbf{x}_{k+1}$ and its associated posterior error covariance $\mathbf{\Sigma}_{xx,k+1}$ as shown in Tab. (1) [28].
In case of colored noises a modification of the KF algorithm based on the spectral factorization theorem has been proposed in [16] which allows to relax the white noise assumption by introducing either (i) correlation of measurement and process noise, (ii) autocorrelated measurement noise or (iii) autocorrelated process noise into the model. Here, the latter case is considered. To this aim, a state space representation of the transfer function $H(\omega)$ in the form

$$\dot{\mathbf{x}}(t) = \mathbf{A}\mathbf{x}(t) + \mathbf{B}u(t) \qquad F(t) = \mathbf{C}\mathbf{x}(t) \tag{30}$$

must be found where the input $u(t)$ is a Gaussian white noise process and the state $\mathbf{x}(t) = [x_1(t), x_2(t), \ldots, x_n(t)]$ is of order n. State-space equations such as Eq. (30) are non-unique. Among the so-called canonical state space models the controllable canonical form is given, setting [29]

$$\mathbf{A} = \begin{bmatrix} -b_0 & -b_1 & \ldots & \ldots & -b_{n-1} \\ 1 & 0 & \ldots & 0 & 0 \\ 0 & 1 & \ldots & \ldots & \ldots \\ \ldots & \ldots & \ldots & 0 & 0 \\ 0 & \ldots & 0 & 1 & 0 \end{bmatrix} \qquad \mathbf{B} = \begin{bmatrix} 1 \\ 0 \\ \ldots \\ \ldots \\ 0 \end{bmatrix} \qquad \mathbf{C} = \begin{bmatrix} a_0 \\ a_1 \\ \ldots \\ a_{m-1} \\ \ldots \\ 0 \end{bmatrix}^T \tag{31}$$

The discretization of Eq. (30) finally leads to the linear state space representation

$$\mathbf{x}'_{k+1} = \mathbf{A}_d \mathbf{x}'_k + \mathbf{B}_d w_k \qquad F_k = \mathbf{C}_d \mathbf{x}'_k \tag{32}$$

which will be used in the following to extend the KF for colored process noise $\{F(t)\}$ with target PSD $S_F(\omega)$. The state space representation of some fundamental stochastic processes such as random bias, first- and second-order Markov process, Brownian motion can be found e.g. in [16]. In [30], the method is applied to introduce a colored process describing the surface roughness of the road into the Kalman filter in order to estimate the states of the vehicle. Comparing Eq. (32) with the state space representation (25) obtained in the previous section by H-FSMs decomposition, the strong resemblance of these two representations is obvious.

3.1 Modification of the Kalman Filter

Following the approach given in [16] the Kalman filter is extended for colored process noise with given PSD by passing a white noise w_k through a linear filter. Augmenting the state vector $\mathbf{x}_{a,k} = [\mathbf{x}_k, \mathbf{x}'_k]^T$ where $\mathbf{x}_k$ are the states of the system and $\mathbf{x}'_k$ represents additional states related to the state space representation of the transfer function $H(\omega)$ of the load process derived either by spectral factorization (32) or by H-FSMs decomposition (25), leads to a state space model

$$\begin{bmatrix} \mathbf{x}_{k+1} \\ \mathbf{x}'_{k+1} \end{bmatrix} = \begin{bmatrix} \mathbf{T}_d & \mathbf{S}_d \mathbf{C}_d \\ \mathbf{0} & \mathbf{A}'_d \end{bmatrix} \begin{bmatrix} \mathbf{x}_k \\ \mathbf{x}'_k \end{bmatrix} + \begin{bmatrix} \mathbf{0} \\ \mathbf{B}_d \end{bmatrix} w_k$$
$$\mathbf{z}_{a,k} = \begin{bmatrix} \mathbf{H}_d & \mathbf{0} \end{bmatrix} \begin{bmatrix} \mathbf{x}_k \\ \mathbf{x}'_k \end{bmatrix} + \begin{bmatrix} \mathbf{v}_k \\ \mathbf{0} \end{bmatrix} \tag{33}$$

which is once again a linear system excited by white noise. Hence, after rewriting Eq. (33)

$$\mathbf{x}_{a,k+1} = \mathbf{T}_a \mathbf{x}_{a,k} + \mathbf{S}_a \mathbf{w}_k \qquad \mathbf{z}_{a,k} = \mathbf{H}_a \mathbf{x}_{a,k} + \mathbf{v}_{a,k} \tag{34}$$

the KF algorithm given in Tab. (1) can be run on the augmented state space model (33) using the modified transfer matrices $\mathbf{T}_a$, $\mathbf{S}_a$ and $\mathbf{H}_a$, respectively.
In order to apply the method for identification problems a further modification is needed in order to estimate the unknown parameters. Following the approach of the extended Kalman filter (EKF), the state $\mathbf{x}_{a,k}$ has to be augmented to include the model parameters $\mathbf{p}_k$ leading to a nonlinear system equation of the extended state $\mathbf{x}_{ext,k} = [\mathbf{x}_{a,k}, \mathbf{p}_k]^T$

$$\mathbf{x}_{ext,k+1} = f(\mathbf{x}_{ext,k}) + \mathbf{S}_{ext} \mathbf{w}_{ext,k} \qquad \mathbf{z}_{ext,k} = h(\mathbf{x}_{ext,k}) + \mathbf{v}_{ext,k} \tag{35}$$

as the system matrices $\mathbf{T}_a$, $\mathbf{H}_a$ depend nonlinearly on the estimates of the state $\mathbf{x}_{a,k}$ and the parameters $\mathbf{p}_k$ known from the previous time step. In case of weak nonlinearities the identification problem is solved using the EKF which linearizes about the current mean and covariance by applying a first order Taylor expansion of Eq. (35) near the current state estimate leading to the time variant extended system matrices $\mathbf{T}_{ext,k}$, $\mathbf{H}_{ext,k}$

$$\mathbf{T}_{ext,k} = \frac{\partial f(\mathbf{x}_{ext,k})}{\partial x_{ext,k}} \qquad \mathbf{H}_{ext,k} = \frac{\partial h(\mathbf{x}_{ext,k})}{\partial x_{ext,k}} \tag{36}$$

to be calculated at each time step. The standard KF algorithm shown in Tab. (1) can be now run on the linearized model: first the prior estimate is calculated by the nonlinear state space model given in Eq. (35), then the update of the error covariances and the measurement update is calculated by introducing the extended system matrices.

3.2 Numerical examples

The proposed method is now applied to a single degree of freedom (SDOF) system excited by the introduced three load cases in order to estimate the stiffness and damping parameter.

1. Exponentially correlated wind gusts:
The first example is taken from [16] and is used in order to show the consistency of the introduced algorithm based on the H-FSMs decomposition and the factorization method introduced there. In this example the (long period) longitudinal dynamics of an aircraft are approximated by the continuous state space model of a harmonic oscillator with natural eigenfrequency $\omega = \sqrt{k/m}$ and ratio of critically damping $D = c/(2m\omega)^{-1}$ given by

$$\dot{\mathbf{x}} = \begin{bmatrix} 0 & 1 \\ -\omega^2 & -2D\omega \end{bmatrix} \mathbf{x} + \begin{bmatrix} 0 \\ 1/m \end{bmatrix} w_c \tag{37}$$

where $\mathbf{x} = [\phi,\ \dot{\phi}]^T$ and ϕ denotes the pitch angle, i.e. the angle between the longitudinal axis of the aircraft and the horizon. The colored process noise w_c represents wind gusts with exponential AC function $R(\tau) = \sigma^2 e^{-a|t|}$. Performing the spectral factorization on the corresponding PSD in Eq. (9) results in the so-called shaping filter $H(s)$, that is the Laplace transform counterpart of the transfer function $H(\omega)$, of the noise $w_c(t)$ in the form

$$H(s) = \frac{\sigma}{a+s} \tag{38}$$

Further details on the spectral factorization can be found in [16, 22]. Using the controllable canonical state space representation in Eq. (31), the shaping filter $H(s)$, given in Eq. (38) corresponds in the time domain to the first order Markov model

$$\dot{x}' = -ax' + w' \qquad w_c = x' \tag{39}$$

which is excited by a Gaussian white noise w' with standard deviation σ. It is used in order to augment the state space model in Eq. (37) leading to

$$\dot{\mathbf{x}}_a = \begin{bmatrix} 0 & 1 & 0 \\ -\omega^2 & -2D\omega & 1/m \\ 0 & 0 & -a \end{bmatrix} \mathbf{x}_a + \begin{bmatrix} 0 \\ 0 \\ 1 \end{bmatrix} w' \tag{40}$$

where $\mathbf{x}_a = [\phi,\ \dot{\phi}, x']^T$ denote the augmented state. After discretization of the augmented model, e.g. by Euler approximation or by using the matrix exponential function, a linear model excited by Gaussian white noise in the form of Eq. (34) is obtained. It will be used in this example for the generation of the 'true' measurement of the pitch angle $\phi(t)$ used in the KF algorithm.
By means of the approach using fractional calculus the augmented state space model is obtained by the following procedure: (i) the system's state space representation is formulated, (ii) the H-FSMs are calculated from the target PSD and the weights β_k of the Gaussian white noise are determined using Eq. (24), (iii) the initial vector $\mathbf{x}'_0$ of increments of Gaussian white noise and the system matrices of the generalized state space model in Eq. (25) are stored and introduced in Eq. (33) to obtain the augmented state space model. In the following, the KF algorithm based on this approach will be indicated as 'H-fractional KF' and the corresponding noise is denoted as 'H-fractional noise', respectively.
The evaluation of the pitch angel and the input force is estimated from out-put only measurements using the H-fractional KF. Fig. (3) depicts the evaluation and AC of the pitch angle $\phi(t)$ (Top) and the corresponding process noise exciting the system (Bottom). In order to illustrate that the KF algorithm not just updates the pitch angle $\phi(t)$ but also the H-fractional noise, the load process is depicted in gray for the case without

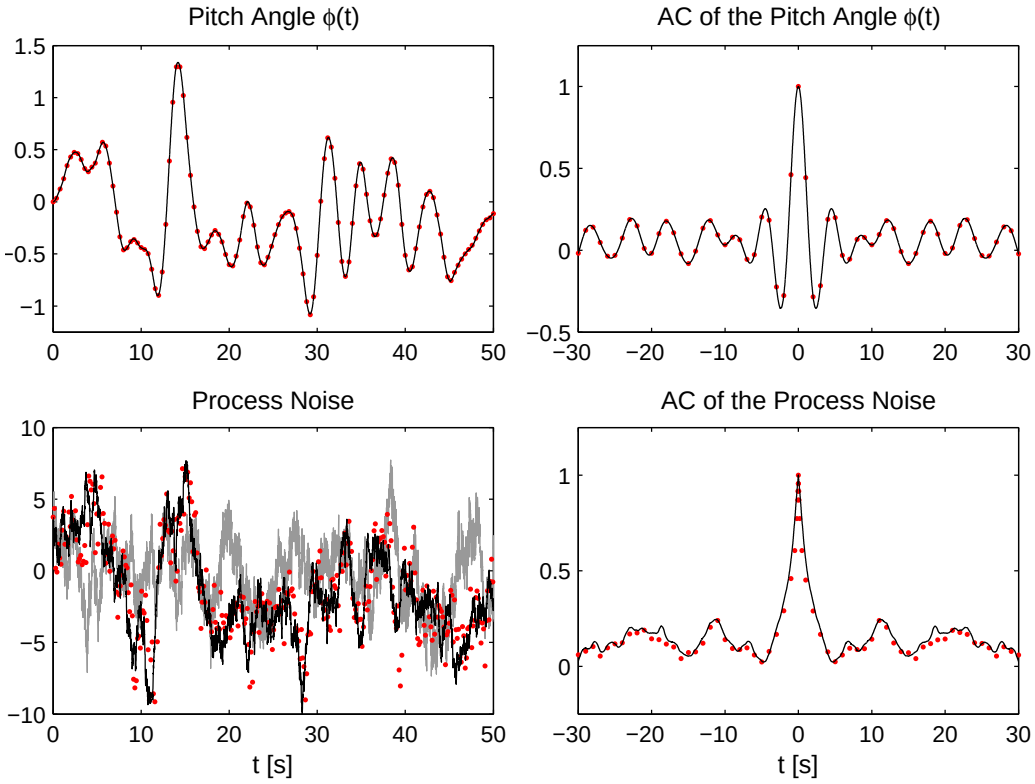

Figure 3: Top: Evaluation of the pitch angle $\phi(t)$ for $\omega = \sqrt{2}$ [rad/s], $D = 0.05$ [-], Bottom: Colored process noise generated by spectral factorization (black), by H-FSMs (gray) and estimated by the fractional KF (red dotted)

consideration of the measurement date and in red after applying the KF algorithm.
In order to estimate the system's stiffness $k = 10$ [N/m] and damping constant $c = 0.707$ [Nm/s] ($D = 0.05$) now the so-called 'H-fractional EKF' is applied. It is assumed that noisy measurement date of the pitch angle $\phi(t)$ and the velocity $\dot{\phi}(t)$ is available taking into account a measurement error of $\sigma_z = 1$ [cm] which corresponds to 1 % of the maximal deflections. It is assumed that a set of 20 measurements of a duration of 10 [min.] each are available. The H-fractional EKF as well as the standard EKF is run on the samples. In the latter case the correlation of the load process is neglected and modeled as white noise with equivalent standard deviation. The initial values of the stiffness and damping parameter $\hat{k}_0$, $\hat{c}_0$ are selected considering an estimation error $\epsilon_{k_0} = |\hat{k}_0 - k|/k$, $\epsilon_{c_0} = |\hat{c}_0 - c|/c$ of 50 %. The mean value as well as the corresponding 90 % confidence intervals of the identified model parameters are depicted in Fig. (4). In case of the H-fractional EKF the stiffness parameter is estimated with high accuracy while the identification of the

case	initial estimate		identified parameters		standard deviation		identification error	
	$\hat{k}_0$ [N/m]	$\hat{c}_0$ [Ns/m]	$\hat{k}$ [N/m]	$\hat{c}$ [Ns/m]	$\sigma_{\hat{k}}$ [N/m]	$\sigma_{\hat{c}}$ [Ns/m]	ϵ_k [%]	ϵ_c [%]
Exponential	5	0.35	9.93	0.79	0.15	0.12	0.7	11.7
von Kármán	5	0.35	10.01	0.82	0.28	0.18	0.1	16.2
Pierson Moskowitz	5	0.35	9.96	0.81	0.20	0.18	0.4	14.6
true values	$k = 10$ [N/m], $c = 0.707$ [Ns/m]							

Table 2: Identification results for the different load cases

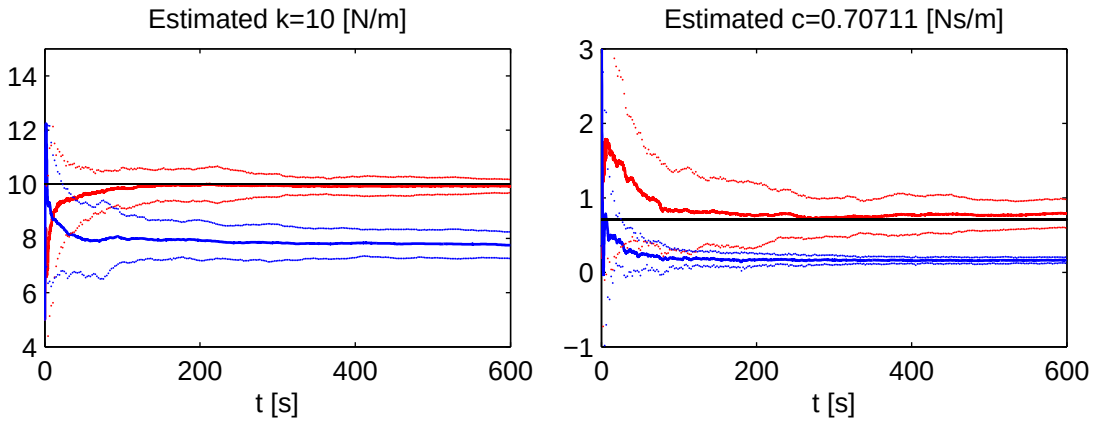

Figure 4: Estimation of the stiffness k [N/m] and damping constant c [Ns/m] of the SDOF system excited by an exponentially correlated load process by means of H-fractional EKF (red) and the standard EKF (blue). The dotted lines represent the corresponding 90 % confidence intervals.

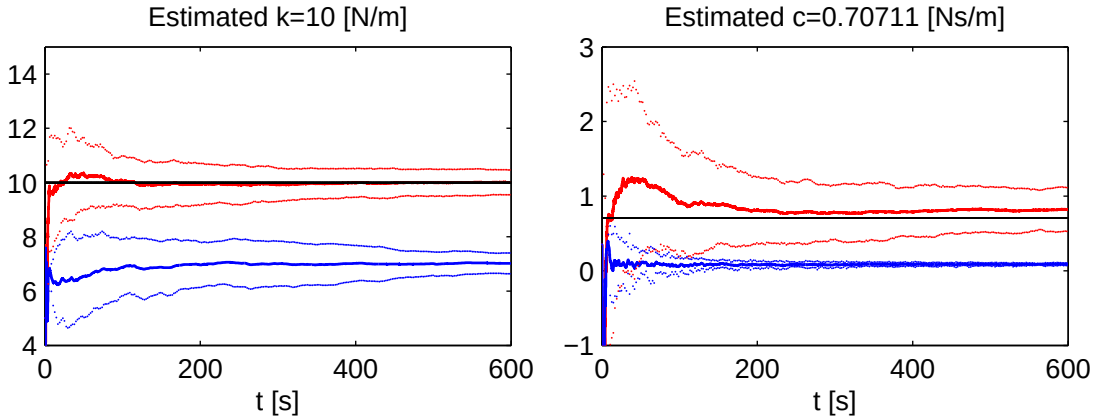

Figure 5: Estimation of the stiffness k [N/m] and damping constant c [Ns/m] of the SDOF system excited by wind loads with von Kármán velocity PSD by means of H-fractional EKF (red) and the standard EKF (blue). The dotted lines represent the corresponding 90 % confidence intervals.

damping parameter leads to an error of 11.7 %. As the damping parameter of weakly damped systems has no significant effect on the modal frequencies and the observed system response of naturally excited systems, the accuracy of the damping estimation is not very high and even in numerical simulations errors of about 20 % are not unusual [31]. Neglecting the correlation of the load process leads to poor identification results as shown by means of the standard EKF which fails to identify both the stiffness and damping parameter. The results of the parameter identification of the H-fractional EKF are summarized in Tab. (2).

2. Wind gusts with von Kármán velocity PSD

As shown in section 2 the corresponding H-FSMs are different, but the implementation of the filter is the same as in the previous example. The results of the parameter identification for the H-Fractional EKF and the standard EKF are illustrated in Fig. (5). Once again the standard EKF leads to poor identification results while the introduced method allows to estimate the stiffness parameter with high and the damping parameter with satisfying accuracy.

3. Wind waves with Pierson-Moskowitz PSD

The results of the parameter identification are shown in Fig. (6). The estimated stiffness and damping parameter corresponds to the generalized quantities of the first eigenmode of a clamped vertical pile which is

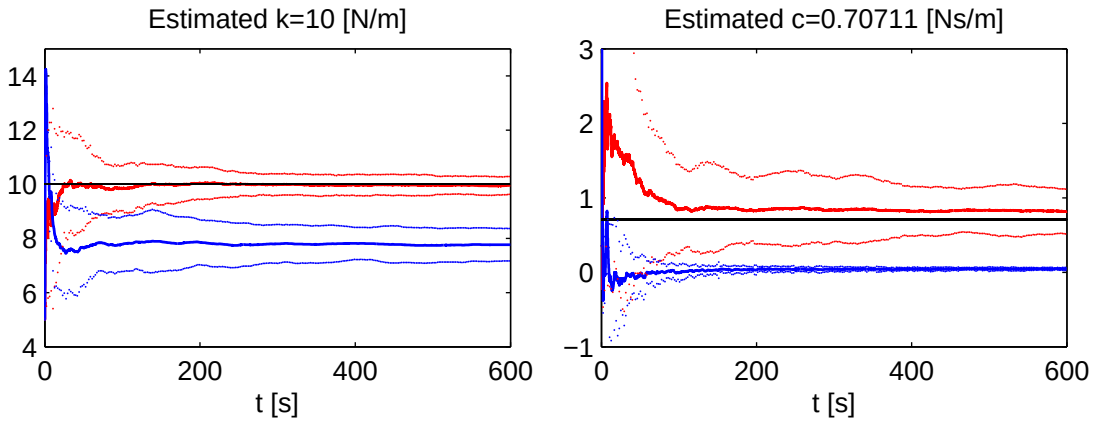

Figure 6: Estimation of the stiffness k [N/m] and damping constant c [Ns/m] of the SDOF system excited by wind loads with P-M PSD by means of H-fractional EKF (red) and the standard EKF (blue). The dotted lines represent the corresponding 90 % confidence intervals.

excited by wind-induced ocean waves. The accuracy of the parameter identification is comparable to the previous examples and the results are summarized in Tab. (2). In contrast to the standard EKF, the uncertainties in the damping estimation are reflected in the high standard deviation of the estimate which leads in all three cases to a relative wide 90 % confidence interval.

4 Conclusions

In this paper we introduced the H-fractional extended Kalman filter for the treatment of arbitrarily autocorrelated load processes in the scope of parameter identification problems.
The system's input was represented as output of a fractional differential equation with white noise as input. In contrast to other techniques, such as the spectral factorization method or ARMA models, the coefficients for the noise simulation are calculated in analytical form from the fractional spectral moments of the linear transfer function. Three load cases of engineering interest have been studied: a process with (i) exponential autocorrelation function and (ii) von Kármán power spectral density, which are extensively used in wind engineering in order to model along wind turbulences, and (iii) with Pierson Moskowitz power spectral density which is widely used in coastal engineering applications for the description of wind induced waves. In all three cases, we succeeded to give the coefficients for the generation of the load processes in analytical form. Furthermore, a generalized state space representation for colored processes have been developed, which can be given immediately, once the H-fractional spectral moments of the transfer function are calculated. Augmenting the state space model of the excited system by the linear model corresponding to the load process, results in an overall linear system driven by white noise once again to which the extended Kalman filter, a commonly used algorithm for recursive parameter identification, can be applied.
This method, indicated as H-fractional extended Kalman filter algorithm, is applied to a SDOF system excited by the three load cases in order to estimate the stiffness and damping parameter using noisy measurement data of the system response. In all examples the stiffness parameter was estimated with high accuracy and the damping parameter was identified with satisfying accuracy.
Most output-only identification techniques represent the systems's input as white noise process. In order to illustrate the effect of such a rough simplification if the white noise assumption is violated, the method was compared with the standard extended Kalman filter. It has been shown that neglecting the autocorrelation of the load process leads to poor identification results for both the stiffness and the damping parameter.

References

[1] S. S. Ivanovic, M. D. Trifunac, T. M. I., Ambient vibration tests of structures: A review, ISET Journal of Earthquake Technology 37 (4) (2000) 165–197.

[2] G. H. James, T. G. Carne, J. P. Lauffer, The natural excitation technique (NExT) for modal parameter extraction from operating wind turbines, Tech. rep., Sandia National Laboratories (1993).

[3] B. Peeters, G. De Roeck, T. Pollet, L. Schueremans, Stochastic subspace techniques applied to parameter identification of civil engineering structures, in: Proceedings of New Advances in Modal Synthesis of Large Structures: Nonlinear, Damped and Nondeterministic Cases, 1995, pp. 151–162.

[4] B. Peeters, G. De Roeck, L. Hermans, T. Wauters, C. Krämer, C. De Smet, Comparison of system identification methods using operational data of a bridge test, in: Proceedings of ISMA 23, International Conference on Noise and Vibration Engineering, Leuven, Belgium, 1998, pp. 923–930.

[5] G. De Roeck, B. Peeters, W.-X. Ren, Benchmark study on system identification through ambient vibration measurements, in: Proceedings 18th Int. Modal Analysis Conference, San Antonio, 2000, pp. 1106–1112.

[6] J. M. W. Brownjohn, Ambient vibration studies for system identification of tall buildings, Earthquake Engineering and Structural Dynamics 32 (2003) 71–95.

[7] W.-X. Ren, Z.-H. Zong, Output-only modal parameter identification of civil engineering structures, Structural Engineering and Mechanics 17 (3-4) (2004) 429–444.

[8] C. Gentile, A. Saisi, Ambient vibration testing of historic masonry towers for structural identification and damage assessment, Construction and Building Materials 21 (2007) 1311–1321.

[9] B. Jaishi, W.-X. Ren, Structural finite element model updating using ambient vibration test results, Journal of Structural Engineering ASCE 131 (4) (2005) 617–628.

[10] S. W. Doebling, C. R. Farrar, Computation of structural flexibility for bridge health moitoring using ambient modal data, in: Proceedings of the 11th ASCE Engineering Mechanics Conference, 1996, pp. 1114–1117.

[11] B. Peeters, J. Maeck, G. De Roeck, Vibration-based damage detection in civil engineering: excitation sources and temperature effects, Smart Materials and Structures 10 (2001) 518–527.

[12] J. W. Lee, J. D. Kim, C. B. Yun, J. M. Shim, Health-monitoring method for bridges under ordinary traffic loadings, Journal of Sound and Vibration 257 (2) (2002) 247–264.

[13] K.-V. Yuen, L. S. Katafygiotis, Bayesian time-domain approach for modal updating using ambient data, Probabilistic Engineering Mechanics 16 (3) (2001) 219–231.

[14] Á. Cunha, E. Caetano, Experimental modal analysis, Sound and Vibrations 40 (6) (2006) 12–20.

[15] M. Prevesto, M. Olagnon, A. Benveniste, M. Basseville, G. Le Vey, State space formulation: a solution to modal parameter estimation, Journal of Sound and Vibration 148 (2) (1991) 329–342.

[16] F. L. Lewis, L. Xie, D. Popa, Optimal and Robust Estimation: With an Introduction to Stochastic Control Theory, Taylor &Francis Group, 2008.

[17] R. E. Kálmán, A new approach to linear filtering and prediction problems, Journal of Basic Engineering (1960) 35–45.

[18] G. Cottone, M. Di Paola, A new representation of power spectral density and correlation function by means of fractional spectral moments, Probabilistic Engineering Mechanics 25 (3) (2010c) 348–353.

[19] G. Cottone, M. Di Paola, R. Santoro, A novel exact representation of stationary colored gaussian processes (fractional differential approach), Journal of Physics A: Mathematical and Theoretical 43 (085002) (2010d) 16–32.

[20] G. Cottone, M. Di Paola, Fractional spectral moments for digital simulation of multivariate wind velocity fields, Journal of Wind Engineering and Industrial Aerodynamics 99 (6-7) (2011) 741–747.

[21] K. Runtemund, G. Cottone, G. Müller, Treatment of arbitrarily autocorrelated load functions in the scope of parameter identification, Computers and Structures (article under review).

[22] P. S. Maybeck, Stochastic models, estimation, and control, Vol. 1 of Mathematics in Science and Engineering, Academic Press, 1979.

[23] A. Bagchi, Rational approximations of the power spectral density of atmospheric turbulence arising in adaptive optics, Tech. rep., University of Twente (2003).

[24] D. D. Holm, Taylor′s hypothesis, hamilton′s principle and the LANS-alpha model for computing turbulence, Los Alamos Science 29 (2005) 172–180.

[25] H. Ruscheweyh, Dynamische Windwirkung an Bauwerken: Praktische Anwendungen, Bauverlag, 1982.

[26] J. Li, J. Chen, Stochastic dynamics of structures, Wiley, 2009.

[27] E. J. Norton, D. C. Quarton, Recommendations for design of offshore wind tubines (RECOFF), Tech. rep., Garrad Hassan and Partners Ltd (2003).

[28] K. Runtemund, G. Müller, Bayesian approach of the skewed Kalman filter applied to an elastically supported structure, in: Proceedings of ISMA, International Conference on Noise and Vibration Engineering, Leuven, 2010.

[29] T. Kailath, Linear systems, Prentice-Hall information and system sciences series, Prentice-Hall, 1980.

[30] W. Jeong, K. Yoshida, H. Kobayashi, K. Oda, State estimation of road surface and vehicle system using a kalman filter, JSME International Journal 33 (4) (1990) 528–534.

[31] R. Ceravolo, Use of instantaneous estimators for the evaluation of structural damping, Journal of Sound and Vibration 274 (2004) 385–401.